EFFECTS OF GF-6 SATELLITE RED-EDGE BANDS ON PEANUT DROUGHT MONITORING

Zhang, Yan[1]; Li, Pei[2]; Liu, Ting [1]; He, Jia [1]; Wang, Laigang [1]; Guo, Yan [1]; Zhang, Hongli [1]; Yang, Xiuzhong [1]
1: Institute of Agricultural Economic and Information· Henan Academy of Agricultural Sciences· Zhengzhou 450002· China;
2: The Fourth Geological Exploration Institute, Henan Bureau of Geo-exploration and Mineral Development, Zhengzhou 450000, China

Commission III, WG III/IVa

KEY WORDS: Remote Sensing, GF-6 WFV, Red-Edge Band, Peanut, Drought, Monitoring.

ABSTRACT:

Red-edge band is an indicator band to describe the health status of crops. In order to explore the impact of the red-edge bands on the accuracy of agricultural drought monitoring, this study used GF-6 WFV and Landsat8 to calculate the Red-edge Normalized Difference Vegetation Index (NDVI705), Vogelmann red-edge index 1 (VOG1), Normalized Difference Vegetation Index (NDVI) and Land Surface Temperature (LST) to construct temperature vegetation drought index (TVDI), this index integrated vegetation index and land surface temperature information, the soil relative humidity data and the measured drought grade data were respectively used for correlation analysis and classification accuracy verification of the TVDI results. The results showed that dry edge equation fit with red edge bands were higher than that of non-red edge bands. The dry edge equation based on VOG1 index has the highest fit, with a maximum coefficient determination of 0.92; TVDI constructed by the above vegetation index have significant negative correlation with soil relative humidity. The TVDI based on the VOG1 index has a better correlation with the relative soil humidity, with a maximum correlation coefficient of 0.85; and realized the dynamic monitoring of peanut drought grade, the overall accuracy rate of peanut drought grade monitoring reached 92.59%, and the result of TVDI classification was in good agreement with the actual drought grade measurement result. The red edge bands of GF-6 satellite can effectively improve the accuracy of peanut drought monitoring and better characterize peanut drought information. This research provides a data reference for the application of GF-6 WFV data in agricultural drought monitoring.

1. INTRODUCTION

In the 21th century, the rapid development of satellite remote sensing technology and near-Earth remote sensing technology provided a new way for drought monitoring [1]. Modern remote sensing can affect the detection of plants through the spectral reflection information of red, green, blue, near-infrared, red edge and other bands received by sensors [2]. growth status was characterized. Studies have shown that when crops are subjected to drought stress [3], the leaf water content [4], leaf area index [5], and chlorophyll content [6] all show a downward trend with the increase of the degree of stress, which can be used as important indicators for evaluating the degree of drought in farmland [7], and the red-edge band (wavelength range 0.69 ~ 0.73 m) is sensitive to the changes of these indicators, and has broad application prospects in crop drought monitoring. Su Wei [8] constructed a regression analysis of multiple vegetation indices and canopy chlorophyll content based on UAV images, and found that the correlation between the vegetation index and chlorophyll content with the participation of the red edge band was high, and the determination coefficient was up to 0.702, the red edge band is sensitive to the change of the chlorophyll content of the maize canopy, and the addition of the red edge band can effectively improve the accuracy of chlorophyll content estimation. Vaz [9] used a portable plant reflectance spectrometer to measure the spectral reflectance of grape leaves and calculated the red edge parameters such as the normalized red edge vegetation index (Red-edge Normalized Difference Vegetation Index, NDVI705), red edge position, etc. The correlation between the relative water content of grape leaves and the red edge vegetation index under soil moisture treatment was analysed. arid variety. Lin Yi [10] used hyperspectral data to study the variation characteristics of the spectral reflectance of maize canopy under different drought stress conditions, and found that the red edge parameter responded quickly to drought stress and could be used as a reference for judging the degree of drought in farmland. The above research has laid a good foundation for the research of red-edge band in agricultural drought remote sensing monitoring. However, most of these studies use hyperspectral near-Earth remote sensing data or UAV remote sensing data, and the scope of application can only be carried out in small areas, and it is difficult to achieve continuous monitoring in large-scale areas.

With the successful launch of satellites with red-edge band such as WorldView-2, WorldView-3, Super Dove, Sentinel-2 and Gaofen-6, it is possible to use the red-edge band to monitor agricultural drought in a large area. Harry West constructed NDVI to invert soil moisture in the southwestern United States by replacing the red band of the Sentinel-2 data with the red band. The results showed that the vegetation index involved in the red band had a high inversion accuracy for soil moisture [11], and higher than the red band. As China's first satellite with a red-edge band sensor, the domestically produced Gaofen-6 satellite has realized the replacement of similar foreign data by domestically produced high-resolution satellite data, breaking the long-term dependence on foreign satellites for medium-resolution and high-resolution data in agricultural remote sensing monitoring. Gaofen-6 has the characteristics of wide coverage, high revisit, high resolution, and multi-spectral characteristics [12], and it satisfies the application requirements of regional-scale agricultural remote sensing monitoring to a higher degree. There have been some applications in agricultural monitoring such as crop growth diagnosis [13], orchard [14], and the newly added red-edge band has improved the monitoring accuracy [15,16]. However, there are few applied studies using the red-edge band of GF-6 satellite data for agricultural drought. Therefore, in this study, Sheqi County, Henan Province was talked as an example, based on GaoFen-6 Wide Field of View (GF-6 WFV) and Landsat8 data, the vegetation index was constructed using the red edge band to determine the relationship between temperature and vegetation drought. Improve the Temperature Vegetation Drought Index (TVDI), carried out remote sensing monitoring

This contribution has been peer-reviewed. The double-blind peer-review was conducted on the basis of the full paper.
https://doi.org/10.5194/isprs-annals-V-3-2022-563-2022 | © Author(s) 2022. CC BY 4.0 License.

research on peanut drought, explore the advantages of GF-6 red-edge band in peanut drought monitoring, and provide reference for the application of GF-6 satellite in agricultural drought monitoring.

Sheqi County is affiliated to Henan Province, China, with a geographical location ranging from 32°47′N to 33°07′N and 112° 45′E to 113°11′E, as shown in Figure 1. The climate of Sheqi County belongs to the transition zone from the north subtropical zone to the warm and humid zone, and has obvious continental monsoon climate characteristics. Peanut was the oil crop with the largest sown area in Sheqi County, second only to wheat. The peanut planting method in this study area was mainly based on direct seeding after wheat is harvested. Generally, it was sown in June and harvested in September. During the period from June 1 to September 9, 2019, Henan Province continued to experience high temperatures and little rainfall, and most areas experienced droughts of varying degrees. The spatial distribution of peanut planting areas in Sheqi County in 2019 was shown in Figure 1.

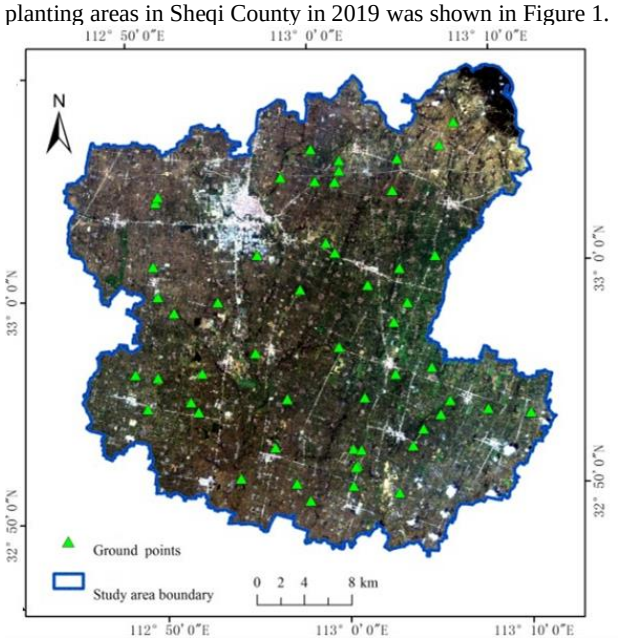

Figure 1. General situation of study area

2. DATA AND METHOD

2.1 Remote Sensing Data

Based on the availability of data, the remote sensing data of GF-6 WFV and Landsat8 satellites on July 7, August 24, and September 9, 2019 were selected, and the cloud cover was less than 5%. GF-6 WFV data are from China Resources Satellite Application Centre (http://www.cresda.com/CN/), with a spatial resolution of 16 m, with B1: blue (0.45 ~ 0.52μm), B2: green (0.52 ~ 0.59μm), B3: red (0.63 ~ 0.69μm), B4: near infrared (0.77 ~ 0.89μm), B5: red edge 1 (0.69 ~ 0.73μm), B6: red edge 2 (0.73 ~ 0.77μm), B7: purple fringe (0.40 ~ 0.45μm), B8: yellow fringe (0.59 ~ 0.63μm) 8 bands. After pre-processing GF-6 WFV with radiometric calibration, atmospheric correction, geometric correction and image cropping with the help of ENVI5.3 image processing software, the normalized difference vegetation index (NDVI) [17], red Table 1 shows the calculation formulas of Red-edge Normalized Difference Vegetation Index (NDVI705) [18] and Vogelmann Red Edge Index 1 (VOG1) [19]. The Landsat8 data comes from the official website of the United States Geological Survey (http: // glovis.usgs.gov/), the image row number is 124/37, and the spatial resolution is 15 m. After resampling to 16 m, the single-window algorithm for the 10th band of Landsat8 TIRS was used to invert the Land Surface Temperature (LST) [20].

Vegetation index	Formula	Bands of GF-6 WFV
NDVI	$\mathbf{NDVI} = (\boldsymbol{\rho}_{\mathbf{NIR}} - \boldsymbol{\rho}_{\mathbf{RED}})/(\boldsymbol{\rho}_{\mathbf{NIR}} + \boldsymbol{\rho}_{\mathbf{RED}})$	B3、B4
$\mathbf{NDVI}_{705}$	$\mathbf{NDVI}_{705} = (\boldsymbol{\rho}_{750} - \boldsymbol{\rho}_{705})/(\boldsymbol{\rho}_{750} + \boldsymbol{\rho}_{705})$	B5、B6
VOG1	$\mathbf{VOG1} = \boldsymbol{\rho}_{740}/\boldsymbol{\rho}_{720}$	B5、B6

Table 1 Vegetation index and its Calculation formula

2.2 Soil Relative Moisture Data

The soil relative humidity data comes from the China Meteorological Science Data Sharing Network (http: // data.cma.cn) "China Meteorological Administration Land Surface Data Assimilation System (CLDAS-V2.0) Real-time Product Dataset", with a spatial resolution of 0.062 5 °×0.062 5°, which is in good agreement with the actual observation value on the ground [21]. This data is used to verify the accuracy of the inversion TVDI. The data selects the 0-20 cm soil relative humidity data in the time period corresponding to the satellite data acquisition period.

2.3 TVDI

The combination of land surface temperature and vegetation index can provide information on surface vegetation and water conditions [22]. When the vegetation coverage in the study area is from bare soil to full coverage, and the soil moisture is from extremely dry to extremely humid, the land surface temperature (LST) is the vertical coordinate, and the scatter plot with the Vegetation Index (VI) as the horizontal coordinate is a triangle [23]. TVDI comprehensively utilizes the information of surface temperature and vegetation index, and its calculation formula is as follows:

$$TVDI = \frac{LST - LST_{min}}{LST_{max} - LST_{min}} \quad (1)$$

Where, LST = surface temperature of any pixel;

LST_{min} =the minimum surface temperature corresponding to the same VI value;

LST_{max} =the maximum surface temperature corresponding to the same VI value.

The TVDI value range is [0, 1]. The larger the TVDI value, the lower the soil moisture and the more severe the drought; on the contrary, the smaller the TVDI value, the higher the soil moisture and the lighter the drought [24]. Using the TVDI index value as the drought grading index, the drought is divided into four grades, namely, 0 ~ 0.6 is no drought, 0.6 ~ 0.7 is mild drought, 0.7 ~ 0.8 is moderate drought, and 0.8 ~ 1.0 is severe drought [25].

2.4 Drought Classification Accuracy

In order to analyse the ability of TVDI to reflect the drought degree of peanuts, referring to the accuracy rate detection method proposed by Liu Dan [26], combined with the measured data of drought level, the accuracy rate of TVDI drought level monitoring results were evaluated. The calculation formula of the accuracy rate is as follows:

$$ACC = \frac{H}{H+M} \times 100\% \quad (2)$$

Where, ACC = the accuracy rate, H = the number of survey points where the TVDI monitoring result is consistent with the ground-measured drought level, M = the number of survey points where the TVDI monitoring result is inconsistent with the ground-level drought level.

3. RESULTS AND ANALYSIS

3.1 LST-VI Feature Space

Using NDVI, NDVI705, VOG1 on July 7, 2019, August 24, 2019, and September 9, 2019, respectively, and the LST of the corresponding date to construct the Land Surface Temperature-Vegetation Index (LST-VI) feature space, and the results are shown in Figure 2. It can be seen from the figure that the scatter distribution shapes of NDVI, NDVI705, VOG1 and LST are all approximately triangular, which is in line with the characteristic space distribution proposed by Sandholt research area.

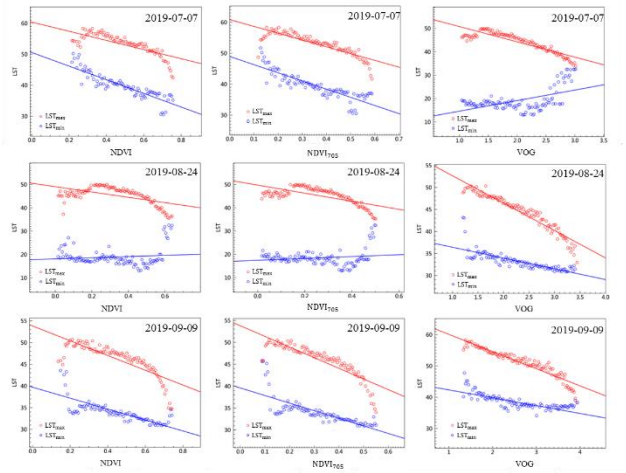

Figure 2. LST-VI spaces from June to September, 2019.

According to the results of different vegetation indices and the characteristic space of surface temperature, the corresponding dry edge and wet edge equations were fitted, and the results are shown in Table 2. It can be seen from the table that when comparing the same period, the R2 of the dry-side equation fitted by the three vegetation indices on August 24, 2019 and September 9, 2019 was larger than the wet-side equation R2; The surface vegetation coverage is low, the red edge information is affected by the underlying surface, and the R2 of the dry edge equation is smaller than the R2 of the wet edge equation. The order of the determination coefficients of the dry-edge equation with different indices is: VOG1>NDVI705>NDVI. The addition of the red-edge band improves the fit of the dry-edge equation. When comparing different periods, the fit of the dry-edge equation was the highest with the VOG1 index, and the coefficient of determination of the dry-edge equation reached 0.92 on September 9, 2019. In addition, the slopes of the dry side are all less than 0, and the slopes of the wet side are all greater than 0, indicating that the maximum surface temperature decreases with the increase of the vegetation index, and the minimum surface temperature increases with the increase of the vegetation index.

Date	VI	Dry Edge Equation	R^2	Wet Edge Equation	R^2
2019-07-07	NDVI	LST_{max}=60.3-14.7 NDVI	0.44	LST_{min}=50.5+22.0 NDVI	0.56
	$NDVI_{705}$	LST_{max}=60.8-21.9 $NDVI_{705}$	0.72	LST_{min}=48.9+26.3 $NDVI_{705}$	0.74
	VOG1	LST_{max}=65.5-5.48 VOG1	0.74	LST_{min}=44.8+2.50 VOG1	0.76
2019-08-24	NDVI	LST_{max}=49.0-11.4 NDVI	0.35	LST_{min}=18.1+2.51 NDVI	0.31
	$NDVI_{705}$	LST_{max}=49.7-17.3 $NDVI_{705}$	0.46	LST_{min}=17.4+3.99 $NDVI_{705}$	0.42
	VOG1	LST_{max}=57.3-6.53 VOG1	0.79	LST_{min}=10.1+4.50 VOG1	0.37
2019-09-09	NDVI	LST_{max}=53.8-17.0 NDVI	0.65	LST_{min}=39.7-1.6 NDVI	0.55
	$NDVI_{705}$	LST_{max}=53.8-24.3 $NDVI_{705}$	0.75	LST_{min}=39.5+17.3 $NDVI_{705}$	0.57
	VOG1	LST_{max}=58.8-6.22 VOG1	0.92	LST_{min}=38.8+2.44 VOG1	0.58

Table2. Equations of dry edge and wet edge of different vegetation index

3.2 Correlation Analysis Between TVDI And Soil Relative Humidity

Through the correlation analysis between 0-20 cm soil relative humidity and TVDI in the corresponding period, the effectiveness of TVDI in monitoring peanut drought was verified. The results are shown in Table 3. It can be seen from the table that when comparing the same period, the TVDI (TVDI_NDVI, TVDI_NDVI705, TVDI_VOG1) obtained by using the three vegetation indices NDVI, NDVI705 and VOG1 were all significantly negatively correlated with soil relative humidity ($P<0.05$), the soil relative humidity showed a downward trend, that is, the higher the TVDI, the lower the soil relative humidity, and the more severe the drought. The order of the correlation coefficients is TVDI_VOG1>TVDI_NDVI705>TVDI_NDVI. The TVDI constructed by adding the vegetation index of the red edge band has a higher correlation with the soil relative humidity and can better represent the drought information. When comparing different indices, the correlations between TVDI_VOG1 and soil relative moisture were the highest in the three periods, and the maximum correlation coefficient was 0.85, which were better than TVDI_NDVI and TVDI_NDVI705 in the same period, indicating that TVDI_VOG1 could better monitor drought information. When comparing different periods, the correlation between TVDI and soil relative humidity was higher on August 24, 2019 than on July 7, 2019 and September 9, 2019, because July 7 was the peanut seedling stage, and the ground cover The soil information affects the expression of the vegetation index; September 9 is the mature period of peanuts, and the peanut vegetation index has a saturation effect; and August 24 is the podding period of peanuts, with vigorous growth and high vegetation coverage, and soil in the vegetation information. The influence of background noise is small, and the correlation between TVDI and soil relative humidity is high.

Date	TVDI_NDVI	$TVDI\_NDVI_{705}$	TVDI_VOG1
2019-07-07	-0.19	-0.24	-0.43*
2019-08-24	-0.49*	-0.63*	-0.85*
2019-09-09	-0.34	-0.43*	-0.48*

Table3. Correlation coefficient between soil relative humidity and TVDI based on different vegetation index

3.3 Accuracy Verification

In order to reduce the influence of cloud and soil background, the three-phase TVDI_VOG1 was synthesized and classified into drought grades by the maximum value synthesis

method. The 12 measured points of no-drought grade are all in the TVDI no-drought grade; 10 of the 11 measured points of the mild drought grade are in the TVDI light drought grade, and 1 is in the TVDI moderate drought grade; 15 of the 18 moderate drought grades are measured. In the TVDI medium drought level, 2 are in the TVDI mild drought level, and 1 is in the TVDI severe drought level; 13 measured points of the severe drought level are all within the TVDI severe drought level. The analysis shows that the overall accuracy rate is 92.59%, and the monitoring accuracy of each drought level exceeds 83.33%. There is no significant deviation between the TVDI drought level classification results and the measured levels. The TVDI_VOG1 drought classification results can be used to effectively monitor peanut drought in the study area.

Drought grade	No drought	Mild drought	Moderate drought	Severe drought
No drought	12	0	0	0
Mild drought	0	10	2	0
Moderate drought	0	1	15	0
Severe drought	0	0	1	13
Accuracy（%）	100	90.90	83.33	100

Table 4. Accuracy of drought grade based on TVDI

5.CONCLUSIONS

The scatter distribution shapes of NDVI705, VOG1 and LST calculated by the red-edge band of the GF-6 WFV satellite are in line with the "triangular" characteristic spatial distribution. The dry edge equation of the VOG1 index has the highest fitting degree, and the maximum coefficient of determination is 0.92; the TVDI constructed by the three vegetation indices has a significant negative correlation with the soil relative humidity, and the TVDI constructed based on the VOG1 index has a better correlation with the soil relative humidity, the maximum correlation coefficient was 0.85; the dynamic monitoring of peanut drought grade was realized. The overall accuracy of peanut drought grade monitoring in the study area was 92.59%, and the TVDI classification results were in good agreement with the measured results of drought grades. The red-edge band of GF-6 satellite can effectively improve the accuracy of peanut drought monitoring and better characterize peanut drought information.

ACKNOWLEDGEMENTS

The work is supported by the Henan Province Key R&D and Promotion Project (Science and Technology Research): Research on Wheat Drought Monitoring and Early Warning Based on Intelligent Remote Sensing in Henan Province（222102110086）.

REFERENCES

[1] Xu Lian. Impact of Drought on China's Agriculture and Its Countermeasures[J]. Guangdong Agricultural Sciences, 2011,38(12):201-203.

[2] Yang Yanying, Mao Kebiao, Han Xiuzhen, et al. Characteristics of Drought Disaster and Its Impact on Grain Production in China from 1949 to 2016[J]. China Agricultural Informatics, 2018, 30(05):76-90.

[3] Chen Yanli, Meng Liangli, Huang Xiaohan, et al. Spatial and Temporal Evolution Characteristics of Drought in Guangxi During Sugarcane Growth Period Based on SPEI[J]. Transactions of the Chinese Society of Agricultural Engineering,2019,35(14):149-158.

[4] Ji Ruipeng, Yu Wenying, Feng Rui, et al. Advance in the Response Process of Crops and Early Identification Technologies to Drought Stress [J]. Journal of Catastrophology, 2019, 34(2): 153-160.

[5] Li Xiaohan, Wu Jianjun, Lü Aifeng, et al. The Difference of Drought Impacts on Winter Wheat Leaf Area Index Under Different CO2 Concentration[J]. Acta Ecologica Sinica,2013,33(9): 2936-2943.

[6] Yuan Xiaokang, Zhou Guangsheng, Wang Qiuling, et al. Hyperspectral Characteristics of Chlorophyll Content in Summer Maize Under Different Water Irrigation Conditions and Its Inversion[J]. Acta Ecologica Sinica,2021,41(2): 543-552.

[7] Gu Yanfang, Ding Shengyan, Chen Haisheng, et al. Ecophysiological Responses and Hyperspectral Characteristics of Winter Wheat (Triticum aestivum) Under Drought Stress[J]. Acta Ecologica Sinica, 2008, 28(6):2690-2697.

[8] Su Wei, Wang Wei, Liu Zhe, et al. Determining the Retrieving Parameters of Corn Canopy LAI and Chlorophyll Content Computed Using UAV Image [J]. Transactions of the Chinese Society of Agricultural Engineering, 2020, 36(19):58-65.

[9] Vaz M, Coelho R, Rato A, et al. Adaptive Strategies of Two Mediterranean Grapevines Varieties (Aragonezsyn, Tempranillo and Trincadeira) Face Drought: Physiological and Structural Responses[J]. Theoretical and Experimental Plant Physiology,2016,28(2):205-220.

[10] Lin Yi, Li Qian, Wang Hongbo, et al. Hyperspectral Characteristics of Spring Maize and the Inversion of Soil Moisture Under Drought Stress[J]. Chinese Journal of Ecology 2016,35(5): 1323-1329.

[11] West H, Quinn N, Horswell M, et al. Assessing Vegetation Response to Soil Moisture Fluctuation Under Extreme Drought Using Sentinel-2[J]. Water (Basel),2018,10(7):838-854.

[12] Liu Jia, Wang Limin, Teng Fei, et al. Typical Application of GF-6 Satellite in Remote Sensing Monitoring of Agricultural Resources[J]. Satellite Applications, 2020(12):18-25.

[13] Liu Baokang, Wang Renjun, You Xiaoni, et al. Extraction of Winter Wheat Area Based on GF6-WFV Remote Sensing Image[J]. Geomatics & Spatial Information Technology, 2021,44(01):1-4.

[14] Jiang Yi, Dong Xiuchun, Wang Xin, et al. Planting Survey of Rape in Sichuan Basin Based on GF-6 Images [J]. Sichuan Agricultural Science and Technology,2020(1):68-70.

[15] Li Yu. Research of Chinese Herbal Medicine Information Extraction Based on Remote Sensing Data of GF-6[J], South China Agriculture,2019,13(20):111-113.

[16] Li Wenjie, Guo Xiaolei, Yang Lingbo, et al. Accurate Recognition of Wine Grapes Using Multi-Feature Optimization Based on GF-6 Satellite Images[J]. Transactions of the Chinese Society of Agricultural Engineering, 2020, 36(18): 165-173.

[17] Wu Hailong, Yu Xinxiao, Zhang Zhenming, et al. Soil Moisture Estimation Model Based on Multiple Vegetation Index[J]. Spectroscopy and Spectral Analysis,2014,34(6):1615-1618.

[18] Gitelson A, Merzlyak M N. Spectral Reflectance Changes Associated with Autumn Senescence of Aesculus hippocastanum L. and Acer platinoids L. Leaves. Spectral

features and Relation to Chlorophyll Estimation[J]. Journal of Plant Physiology,1994,143(3):286-292.
[19] Vogelmann J E, Rock B N, Moss D M. Red Edge Spectral Measurements from Sugar Maple Leaves[J]. International Journal of Remote Sensing,1993,14(8):1563-1575.
[20] Hu Deyong, Qiao Kun, Wang Xingling, et al. Land Surface Temperature Retrieval from Landsat 8 Thermal Infrared Data Using Mono-Window Algorithm[J]. Journal of Remote Sensing,2015,19(6):964-976.
[21] Li Chao, Li Xuemei, Tian Yalin, et al.Time and Space Fusion Model Comparison of Temperature Vegetation Drought Index[J] .Remote Sensing Technology and Application, 2020, 35(4): 832-844.
[22] GB/T3136—015, Grade of agricultural drought[S].
[23] Qin Z, Karnieli A, Berliner P. A Mono-Window Algorithm for Retrieving Land Surface Temperature from Landsat TM Data and Its Application to the Israel-Egypt Border Region[J]. International Journal of Remote Sensing,2001, 22(18):3719-3746.
[24] Liu Liyang, Liao Jishan, Chen Xiuzhi, et al. The Microwave Temperature Vegetation Drought Index (MTVDI) Based on AMSR-E Brightness Temperatures for Long-Term Drought Assessment Across China (2003—2010) [J]. Remote Sensing of Environment,2017,199(15):302-320.
[25] Sun Lijun, Liu Xiao, Zhu Yanhuang. Study on the Inversion of Drought Degree in Henan Province Based on MODIS Data[J]. Geomatics & Spatial Information Technology, 2021,44(03):140-142.
[26] Liu Dan, Feng Rui, Yu Chenglong, et al. Remote Sensing Monitoring of Drought Response of Spring Maize Based on Vegetation Indexes[J]. Transactions of the Chinese Society of Agricultural Engineering,2019,35(20):152-161.
[27] Sandholt I, Rasmussen K, Andersen J. A simple interpretation of the surface temperature/vegetation index space for assessment of surface moisture status[J]. Remote Sensing of Environment,2002,79(2/3):213-224.
[28] Wu Zemian, Qiu Jianxiu, Liu Suxia, et al. Advances in Agricultural Drought Monitoring Based on Soil Moisture [J]. Progress in Geography,2020,39(10):1758-1769.
[29] Bai Yanying, Gao Julin, Zhang Baolin. Monitoring of Crops Growth Based on NDVI and EVI[J]. Transactions of the Chinese Society for Agricultural Machinery,2019,50(09):153-161.
[30] Yan Na, Li Dengke, Du Jiwen, et al. Monitoring of Drought Situation in Shaanxi Province Based on MODIS Land Product LST/NDVI and EVI[J]. Journal of Natural Disasters,2010,19(4):178-182.
[31] Wu Manchun, Ding Jianli, Wang Gaofeng. Regional Soil Moisture Inversion Based on Surface Temperature and Vegetation Index Characteristic Spaces[J]. Journal of Desert Research,2012,32(1):148-154.
[32] Chen Mingxing, Zhang Yuhu. Retrieval of Soil Moisture in Sanjiang Plain Based on TVDI Model with Four Vegetation Indices[J] Research of Soil and Water Conservation,2019,26(3):93-100.
[33] Zhang Qinyu, Li Zhe, Xia Chaozong, et al. Tree Species Classification Based on the New Bands of GF-6 Remote Sensing Satellite[J]. Journal of Geo-information Science,2019,21(10):1619-1628.